JOURNAL OF Materials Feature Article CHEMISTRY

Cholesterol-based functional tectons as versatile building-blocks for liquid crystals, organic gels and monolayers

Seiji Shinkai*[a] and Kazutaka Murata[b]

[a]*Department of Chemical Science & Technology, Faculty of Engineering, Kyushu University, Fukuoka 812, Japan*

[b]*CHEMIRECOGNICS Project, ERATO, Research Development Corporation of Japan, 2432-3 Aikawa-cho, Kurume, Fukuoka 830, Japan*

This review article introduces the application of the cholesterol moiety, which has been commonly utilised as a versatile building block in liquid crystals, organic gels and monolayers, to molecular recognition. Effort has especially been made to clarify the characteristics of cholesterol-based assembly systems and the phenomena common to these three systems.

Cholesterol is a well-known natural product and frequently appears as a building block in molecular assemblies. Its versatility stems from its unique structural characteristics not found in other compounds. (1) It is commercially available as a cheap natural product; (2) its structure is rigid and possesses multiple chiral carbon atoms which are prerequisites for chiral recognition;[1] (3) its derivatives can form several unique aggregates such as liquid crystals, organic gels and monolayers; (4) the absolute configuration of C-3 can be easily inverted. Factor (3) in particular most clearly characterises the nature of cholesterol as a building block. Cholesteric liquid crystals are aggregates composed of chirally-oriented planes; organic gels are fibrous (mostly one-dimensional) aggregates which are capable of gelatinizing organic media; monolayers are two-dimensional aggregates formed at the air–water interface. To the best of our knowledge, cholesterol is the only compound that can provide so many different mesophases.[2] Our present research interest is in molecular recognition combined with supramolecular systems. It thus occurred to us that oriented molecular assemblies based on cholesterol aggregates might be useful in molecular recognition processes difficult to attain with other monomeric host compounds. For example, the cholesterol–cholesterol interaction may be affected by guest molecules intercalated between them or by host–guest interactions with the host moiety appended to the cholesterol skeleton. These chemical signals should affect the orientation and/or the pitch length in the cholesterol stack, which can eventually be read out as a change in the spectroscopic properties (*i.e.* physical signals).

In this review article we survey cholesterol-based assemblies (liquid crystals, organic gels and monolayers at the air–water interface) with potential in the design of novel molecular recognition systems.

Liquid crystal systems

Differentiation by colour should be the *magnum opus* of chiral discrimination. In homogeneous solutions this idea has been realised in chromogenic chiral crown ethers and calixarenes.[3] For example, Kaneda *et al.* employed chiral azophenolic acerands in which chiral point interactions can be directly 'read' by a colour change.[3a,b] Our method is somewhat different and employs a chiral environment as outlined in the introduction. The use of cholesterol as a chiral environment is not a new idea: many people have studied and attempted to control chiral reactions in liquid crystals,[4,5] but control of chiral reactions in the cholesteric chiral medium has met with only mediocre success.[5] With our approach, we do not try to control the guest but allow the guest to control the chirality of its environment.

Steroidal crown compounds have been synthesised by several groups and their liquid crystalline properties and membrane-forming properties have also been studied.[6,7] To the best of our knowledge at the beginning of this study, few groups had attempted to apply this system to molecular recognition. Our first foray into the realm of environmental amplification employs cholesteric crown ethers **1**. A mixture of cholesteryl nonanoate and cholesteryl chloride is known as a room temperature cholesteric liquid crystal and generates visible reflected light because the pitch length is comparable to the wavelength of visible light. A ternary blend of cholesteryl nonanoate, cholesteryl chloride and **1** (*ca.* 25 mol%) changes its helical pitch length upon addition of alkali metal salts and, therefore, its colour.[8] Since the pitch length change is dependent on the size of added alkali metal cations, one can easily detect the metal cations from the visible colour change.[8] The results indicate the potential to apply cholesteric liquid crystals as a new metal sensory system. Interestingly, the pitch length for **2** was scarcely affected by addition of these metal cations.[8] This means that if a spacer is inserted between the metal-binding site and the liquid-crystal-forming site, the event occurring at the metal-binding site is absorbed by the flexible molecular segment in the spacer.

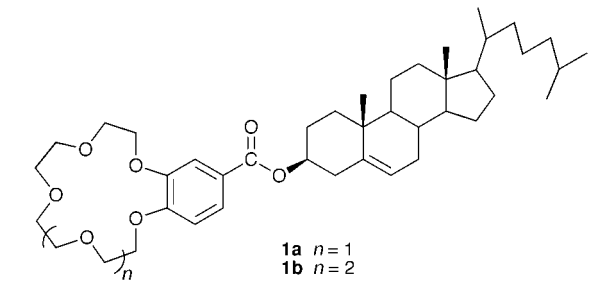

1a $n = 1$
1b $n = 2$

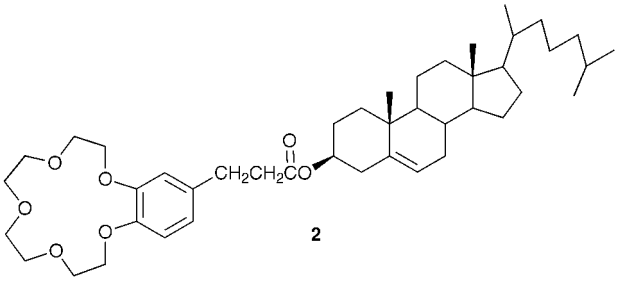

2

* E-mail seijitcm@mbox.nc.kyushu-u.ac.jp

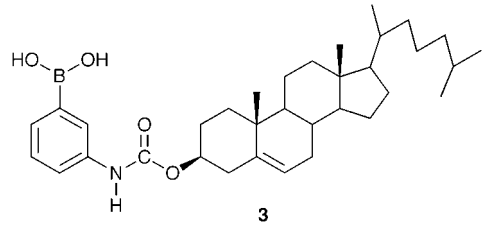

3

As the helical pitch of the mixed cholesteric liquid crystal is chiral, this system may be applicable to chiral molecular recognition. It was found that alkali (*R*)- and (*S*)-mandelates can change the helical pitch in an enantioselective manner.[9] The largest reflectance wavelength maximum (λ_R) difference between (*R*) and (*S*) (69 nm) was observed for the combination of **1b** and potassium salts, which could be visually differentiated [green for (*R*) and blue for (*S*)].[9] On the other hand, such a colour change was not observed for either the combination of **1b** and Bu_4N^+ mandelates or for the combination of **2** and potassium mandelates.[9] The more straightforward chiral recognition with ternary cholesteric liquid crystals was achieved for optically-active ammonium ions through the RNH_3^+–benzo-18-crown-6(**1b**) interaction.[10] In α-amino acid ester derivatives, the λ_R for D-isomers shifted to longer wavelength whereas that for L-isomers shifted to shorter wavelength (except alanine methyl ester hydrochloride which has the smallest residual group). The largest λ_R difference was observed for phenylalanine methyl ester hydrochloride (+45 nm for D-isomer and −19 nm for L-isomer).

With saccharides and cholesterol boronic acid **3** similar doping experiments were carried out and produced similar colour changes.[11] Since the interaction of boronic acid with saccharides produces a cyclic boronate ester, this covalent linkage allows us to isolate the complexes. Once the complexes are isolated the opportunity exists to examine structure–activity relationships. Such an opportunity was not available with alkali metals and ammonium ions. Solvent extraction of saccharides was carried out at 25 °C using solid–liquid ($CDCl_3$) extraction. As much by serendipity as by design **3** was a much more efficient saccharide extractor than the lipophilic boronic acids previously used;[12] complete extraction was observed for all monosaccharides. Selection within the saccharides similar to that previously observed was seen in the rate of extraction, the less favourable saccharides taking longer to be completely extracted. However, after 48 h all the saccharides investigated were completely extracted.[11]

Characterisation of the extracted saccharides could be achieved employing just ^{1}H NMR spectroscopy ($CDCl_3$).[11] The molar ratio of the extracted species could be conveniently estimated by the integral intensities of selected proton resonances of the monosaccharide *versus* either the phenyl or the alkenyl protons of compound **3**. In the case of the D-fucose complex the anomeric proton of the monosaccharide at δ 5.9 and the alkenyl proton of compound **3** at δ 5.4 were employed. In general, all the saccharides form a 1:2 complex with compound **3**. Two main structural classes exist for the extracted monosaccharides; either two five-membered rings are formed (1,2–3,4 complex) or a five- and a six-membered ring are formed (1,2–4,6 and 2,3–4,6 complexes: Scheme 1).

trans-Six-membered rings are less stable than the five-membered ring.[13] From Fig. 1 it can be seen that this structural analysis falls short of describing the actual situation. Some systems that could have formed perfectly good five-membered rings opt for the six-membered ring alternative. Why do these systems prefer the six-membered ring? With galactose and talose the ring is a *cis* rather than a *trans* six-membered one, and it is known from decalin that the *cis* fused six-membered ring system is conformationally flexible whereas the *trans* system is fixed. This conformational lability may provide enough advantageous entropic energy to tip the balance in favour of the six-membered ring. With allose and mannose a *trans* six-membered ring is formed, but this may not be an inherent preference for the six-membered ring but rather a preference for the 2,3 five-membered ring over the 1,2 five-membered ring. In a 1:2 complex once the 2,3 five ring has been formed, the only choice remaining is the formation of a *trans* six-membered ring.

The induced shifts produced by the extracted monosaccharides in a cholesteryl nonanoate–cholesteryl chloride composite liquid crystal are given in Table 1. An example for the visible colour change is shown in Fig. 2. Analysis of Table 1 shows that saccharides with similar structural features induce shifts in the same sense (Fig. 1).[11] Within the saccharides extracted three such structure–shift group relationships exist: the first group includes saccharides with two (*cis*) five-membered boronate ester rings (Group I). When the first ring (following normal saccharide numbering) is down with respect to the saccharide plane and the second ring is up, a red shift is induced (D-fucose and L-arabinose). Conversely, when the first ring is up and the second is down, a blue shift is induced (D-fructose, D-arabinose and L-fucose). The next structure–shift sub-group contains saccharides with one *cis* five-membered ring and either a *trans* five- or a *trans* six-membered ring

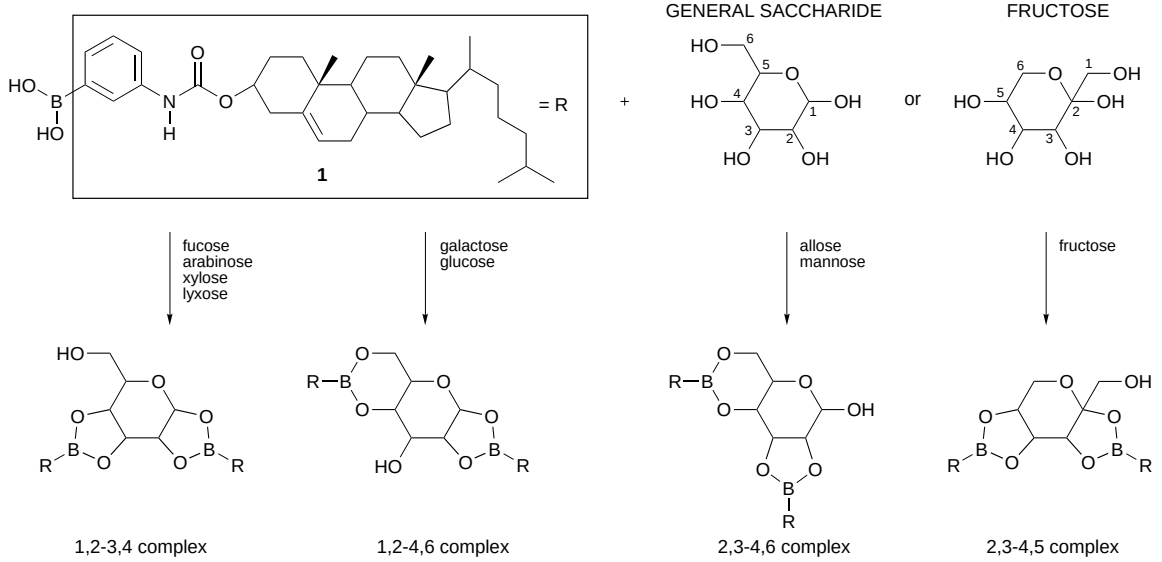

Scheme 1 Structures of 2:1 complexes (**3**–monosaccharide)

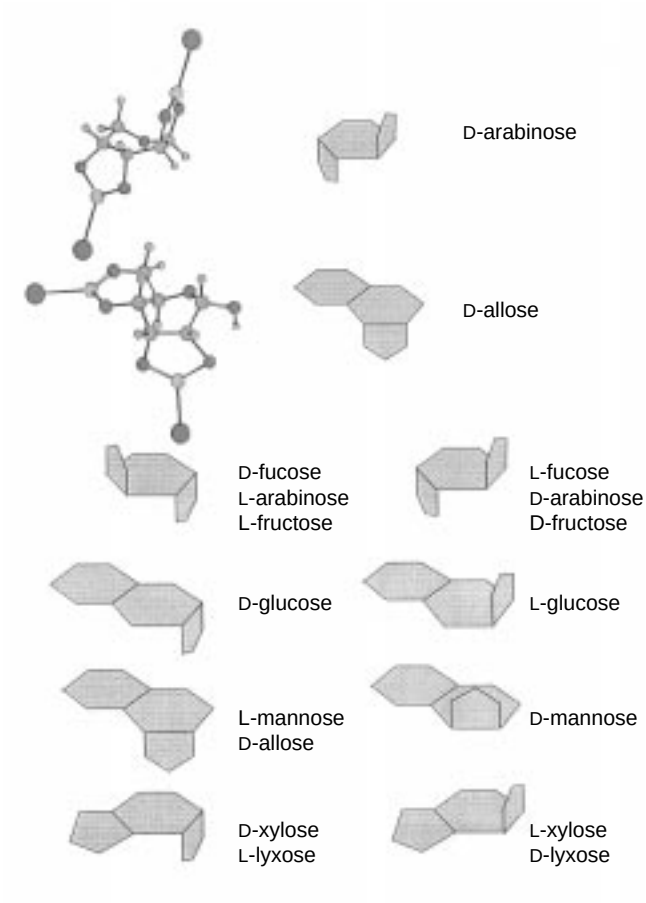

Fig. 1 Cartoon representation of 2:1 complexes: the central hexagon denotes the pyranose ring

(Group II). When the first ring (*cis* five-membered) is down, a red shift is induced (D-glucose, D-allose and D-xylose) and conversely when this ring is up, a blue or no shift is induced (L-glucose and D-mannose). The final structure–shift group is the most anomalous; the saccharide contains both a *cis* five-membered ring and a *cis* six-membered ring (Group III). When the first ring is either up or down, a blue shift is induced (D-galactose and L-galactose), but D-talose induces no shift. This anomalous behaviour may be a result of the conformational lability of the *cis* six-membered ring, or as explained below the

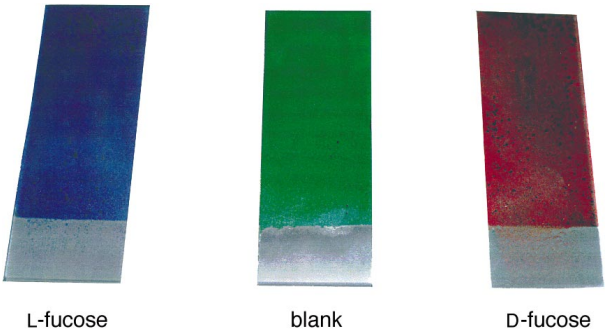

Fig. 2 Visible colour change induced by a **3**·fucose 2:1 complex

behaviour may not be anomalous if a threshold must be overcome before a shift in the pitch occurs.

From the above qualitative structural analysis and the result that the 1:1 complex of 2-deoxy-D-galactose causes no shift, the spatial disposition of two cholesteryl boronic acid moieties is the driving force for the change in the cholesteric pitch. Structural analysis of the complexes utilising a molecular orbital calculation reveals a quantitative relationship between the magnitude and direction of the induced shift and the angle between the phenyl planes of the two boronic acid moieties (Fig. 3). For the correlation depicted in Fig. 3, one apparent anomaly needs to be clarified. Why are blue shift additives 'effective' at all angles, but those compounds inducing a red shift have a threshold value of about 40° (D-fructose)? This can be easily explained by the inherent twist of the support liquid crystal; complexes that add to this inherent twist cause blue shifts, and those that subtract cause red shifts, with D-fructose (40°) acting as the effective zero or threshold.

The foregoing findings demonstrate that the pitch length in cholesteric liquid crystals is useful not only for size recognition of metal cations but also for chiral recognition of natural products. Furthermore, it is noteworthy that the recognition events can be detected by a visible colour change.

Polymer–liquid crystal composite membrane systems

Biological membranes are composed of various kind of phospholipids, cholesterols and proteins, and the fundamental functions such as permeation and selectivity are closely associated with the gel–liquid crystal phase transition. Therefore, the phase transition would be one of the most essential functions

Table 1 Shifts in the reflection light maxima (λ nm) caused by added 2:1 complex: **3**–saccharide[11]

		induced shift[a] relative to compound **3**	
group	2:1 complex **3**–saccharide	mol% 2.4[b]	mol% 1.2[c]
I	D-fucose		123±13
	L-arabinose		27±8
	L-fucose	−164±12	−95±6
	D-arabinose	−82±10	−45±6
	D-fructose	−37±11	−23±11
II	D-glucose	91±10	42±12
	D-allose	69±10	19±10
	D-xylose		34±15
	L-glucose	−71±10	−61±6
	D-mannose	−3±10	5±6
III	D-galactose	−44±10	−33±11
	L-galactose	−17±10	−21±7
	D-talose	3±11	
blank	2-deoxy-D-galactose	6±15	

[a]Shifts are the average of five repeats; errors given are the maximum deviation from the mean. [b]At 2.4 mol% compound **3** has a base reflectance of 625±10 nm. [c]At 1.2 mol% compound **3** has a base reflectance of 650±6 nm.

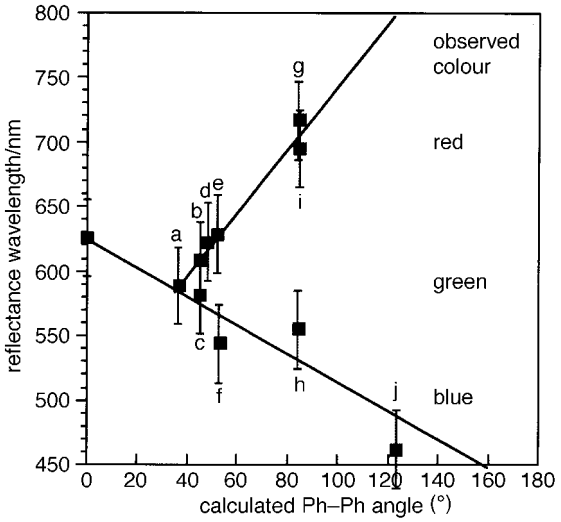

Fig. 3 Plots of reflectance wavelength (λ_R) *vs.* calculated Ph–Ph dihedral angle for 2 : 1 complexes. Saccharides used: a, D-fructose; b, L-galactose; c, D-galactose; d, D-mannose; e, L-arabinose; f, D-arabinose; g, D-glucose; h, L-glucose; i, D-allose; j, L-fucose.

provided by phospholipid membranes. Kajiyama and co-workers[14–16] demonstrated that composite membranes in which the liquid crystalline material is embedded in a polymer matrix are applicable to membrane mimetic permeation control, because a distinct change in the thermal molecular motion occurs at the crystal–liquid crystal phase transition temperature. For example, in ternary composite membranes composed of a polymer (polycarbonate, PC), a liquid crystal (**4**: crystal–nematic liquid crystal phase-transition temperature, 305 K) and crown ethers having a fluorocarbon chain (**5**) K^+ transport is 'completely' suppressed below 305 K whereas K^+ is transported rapidly above 305 K.[16] The results imply that ion permeation across these membranes is drastically affected by the fluidity of the membrane medium.

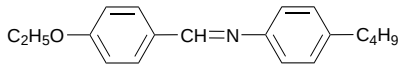

4

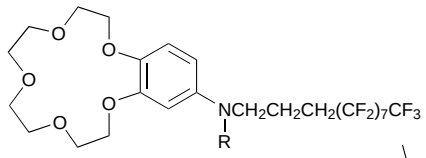

5

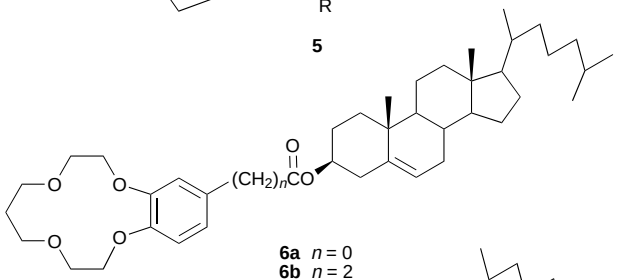

6a $n = 0$
6b $n = 2$

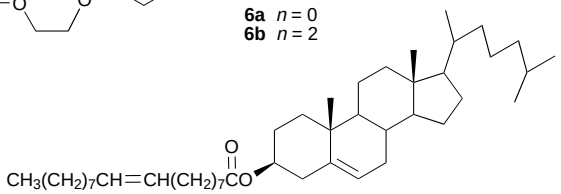

7

If steroidal crown compounds are appropriately embedded in a polymer matrix and the stacked crown column is formed, it is expected to act as a sort of ion channel. The cholesteric liquid-crystal phase of steroidal crown ethers usually appears above 100 °C. It was found, however, that a mixture of **1a** and **1b** or **1a** and **2** results in the cholesteric liquid-crystal phase even at room temperature.[17,18] A composite membrane composed of **1a**, **2** and Perplene [a random copolymer consisting of oxytetramethyleneoxyterephthaloyl and poly(oxytetramethylene)oxyterephthaloyl units] permeated alkali thiocyanates and the rate of ion permeation was in the order $Na^+ > K^+ > Cs^+$.[17] This order is identical with the metal affinity of benzo-15-crown-5. On the other hand, when a mixture of **1a** and **1b** was used, the order was changed to $K^+ > Na^+ > Cs^+$.[18] Obviously, this is due to the contribution of **1b** which shows the highest affinity for K^+.

The ion permeation selectivity of these membranes was further examined using **1**, **2** and **6**.[19] Compound **6b** provided a stable cholesteric mesophase even at room temperature and the composite membrane showed remarkably high Li^+ selectivity. A similar result was obtained from a **6a**–**6b** mixture. A **1a**–**6a** mixture still kept the high Li^+ selectivity, whereas a **1a**–**2** mixture showed the selectivity order of $Na^+ > K^+ > Cs^+ > Li^+$. The results imply that in the mixed systems the crown ether with the smallest ring size acts as a critical 'gate' for ion permeation: that is, **6** allows Li^+ to pass through the benzo-13-crown-4 ring but does not allow Na^+ to do so.

It was proposed that ion permeation in these systems occurs according to an ion-channel mechanism but not according to an ion-carrier mechanism.[18,19] The first evidence for this proposal is the activation energy for the Arrhenius plots (*ca.* 27.3–48.7 kJ mol^{-1}). These values are consistent with the ion-channel mechanism which includes an ion translocation process. In fact, very similar values have been obtained for natural and artificial channel-forming compounds.[20,21] In contrast, the ion-carrier mechanism is known to need a higher activation energy (90–120 kJ mol^{-1}).[22,23] The second piece of evidence is obtained from dilution of the membrane with nonionophoric cholesterol derivatives. For example, when crown-containing cholesterols were diluted with **7** which provides the cholesteric liquid-crystal phase at room temperature, ion permeation was strikingly suppressed. If ion permeation occurs according to the ion-carrier mechanism, the rate should gradually decrease with increasing concentration of **7**. The construction of an ion channel was further corroborated through the ion-conducting behaviour.[24] In composite films with Li^+ or Na^+ salts, the activation energy for ion conduction was lower under the cholesteric liquid-crystal conditions than under the corresponding isotropic conditions. The finding indicates that the crown rings ordered in the cholesteric liquid-crystal phase contruct a channel-like array and facilitate specific ion conduction. It was also shown that in the composite film containing a small amount of **8a**, significant photoinduced ion-conductivity switching is realized by alternate irradiation with UV and VIS light.[24] This phenomenon is attributed to the order–disorder cycle of the liquid crystal state induced by *cis–trans* photoisomerisation of the azobenzene moiety.

The foregoing references reveal that cholesteric liquid crystals are useful not only for the orientation of appended functional groups but also as a medium to selectively permeate guest cations. As mentioned in the previous section, the pitch length of cholesteric liquid crystals changes enantioselectively in response to chirality of intercalated guest molecules. We thus believe that cholesterol-based membranes are effective for chiral separation of racemic compounds.

Gel systems

Recently, a new class of cholesterol-based gels, held together by weak hydrogen bonding or van der Waals interactions, was reported.[25–33] Our interest was sparked, since we have previously nurtured cholesterol derivatives bearing crown ether, azobenzene or boronic acid moieties.[8–11,17–19,24,34] Our continuing theme is the development of signal-responsive

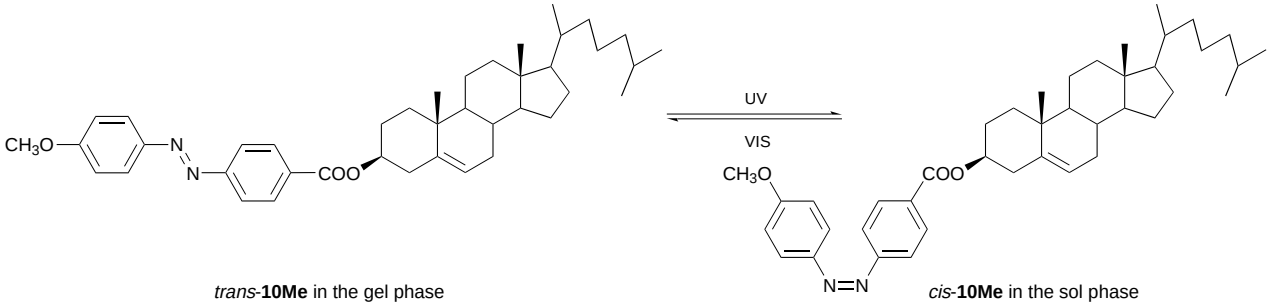

Scheme 2 Sol–gel phase transition induced by photoisomerisation of **10Me** in butan-1-ol

chemistry, employing molecular transducers capable of translating host–guest interactions into readable outputs. Gelation has provided us with a new medium in which we can further explore such interactions. We met with an early success; the sol–gel phase transition temperature (T_{gel}) can be controlled by both metal cations and photo-isomerisation of the azobenzene moiety.[35,36] For example, **8b** can gelatinize a mixed solvent of methylcyclohexane–benzene (4 : 1 v/v). Since alkali metal and ammonium salts are scarcely soluble in the gelation solvent, these metal salts should be solubilised through complexation with the crown ring. The T_{gel} in the presence of Li^+, Na^+, K^+, Rb^+ and NH_4^+ rose with increasing metal or ammonium concentrations whereas that in the presence of Cs^+ decreased.[35,36] Conceivably, the Cs^+ ion which tends to form a 1 : 2 metal–crown sandwich complex with 18-crown-6 effectively disorders the aggregation structure of **8b**. On the other hand, a variety of azobenzene-containing cholesterol derivatives (**9**, **10R** and **11R**) were synthesized and some of them were shown to be useful for photo-control of the sol–gel phase transition.[35,36] For example, butan-1-ol is gelatinized in the presence of only 0.1 mass% **10Me**. When the gel was photoirradiated by a high-pressure Hg-lamp through a VIS-cut colour glass filter ($330 < \lambda < 380$ nm: the *trans*-to-*cis* isomerisation is induced), the gel phase was changed to the sol phase. The gel phase was re-generated when the sol was photoirradiated through a UV-cut colour glass filter ($\lambda > 460$ nm: the *cis*-to-*trans* isomerisation is induced). Hence, the sol–gel phase transition could be controlled reversibly by a light switch (Scheme 2).

As mentioned in the preceding section cholesterol-bound saccharides have a dramatic influence on the pitch length in mixed cholesteric liquid crystals.[11] Addition of 2 or 3 mol% of the 2 : 1 saccharide complex to a composite liquid crystal membrane alters the pitch length in a direction relative to the absolute configuration of the complexed saccharide. This change could be read-out by eye as a colour change in the liquid crystal.[11] It occurred to us that these complexes might act as gelators of organic solvents. If so, one can obtain a variety of 'chiral' gelators by just changing the saccharide source. The gelation test was carried out as follows: the complexes (0–5 mass%) were mixed with solvent in a septum-capped test tube and the mixture was heated until the solid was dissolved.[37] The solution was cooled to room temperature (G in Table 2 denotes that a gel is formed at this stage). When a gel was not formed at room temperature, the solution was cooled in a refrigerator (at $-6\,^{\circ}C$) for one day (Gc in Table 2 denotes that a gel was formed at this stage). The results are summarised in Table 2.[37] Inspection of Table 2 reveals an interesting general trend: optical pairs of saccharides lie at different points along a path of increasing molecular interaction; the path from solution to crystallinity. From our previous work with composite liquid crystal membranes red shift complexes increase the pitch length and blue shift complexes decrease the pitch length of the liquid crystal membrane. Obviously, factors that work to increase the pitch length act to reduce the molecular interaction; likewise a decrease in the pitch length can be correlated with an increase in molecular cohesion. With carbon tetrachloride as solvent the following

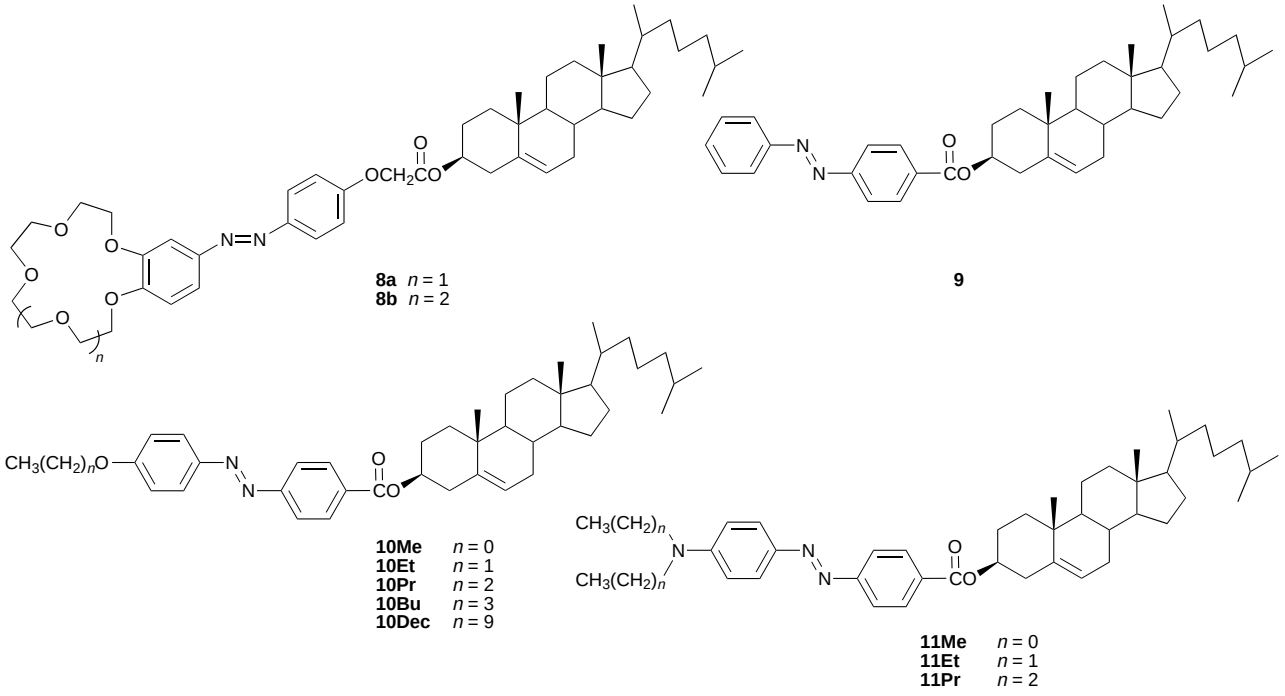

Table 2 Results of the gelation tests carried out with monosaccharide complexes[a]

	lyxose		xylose		mannose		glucose		galactose	
	D-	L-	D-	L-	D-	L-	D-	L-	D-	L-
solvent	blue[b]	red[b]	red[b]	blue[b]	blue[b]	red[b]	red[b]	blue[b]	blue[b]	red[b]
hexane	SW	SW	I	I	I	I	I	I	I	I
benzene	G	G	G	G	S	R	S	I	G	G
toluene	G	G	G	G	I	G	S	I	G	G
dichloromethane	G	G	G	I	I	Gc	S	I	G	Gc
chloroform	G	G	G	G	Gc	G	S	I	S	S
carbon disulfide	G	G	G	SW	G	G	I	I	S	S
diethyl ether	I	S	SW	I	R	S	I	I	S	S
tetrahydrofuran	S	S	S	S	I	S	I	I	S	S
1,4-dioxane	G	S	S	G	S	S	S	S	S	S
ethyl acetate	S	S	R	R	S	S	R	I	S	S
acetone	R	S	R	R	R	R	R	R	I	R
methanol	R	R	R	I	I	I	I	I	I	I
ethanol	S	S	S	I	R	R	R	I	R	R

[a][Gelator] = 0.1–5 mass%; Gel formed when cooled to 23 °C (G) or cooled in a refrigerator to −7 °C (Gc); Gel not formed because of crystallisation (R), soluble (S), or insoluble (I); SW = swollen. R means that the gelator is soluble at high temperature and precipitated at 23 °C whereas I means that the gelator is not soluble even at high temperature. [b]Colour induced in a composite liquid crystal membrane.

occurred: L-lyxose (gel), D-lyxose (insoluble); D-xylose (gel), L-xylose (insoluble); L-mannose (gel), D-mannose (insoluble); D-glucose (solution) and L-glucose (recrystallises). For the chiral pairs of complexes the former are predicted to have weak cohesion from the liquid crystal work (red shift), and the latter strong intermolecular cohesion (blue shift). This prediction clearly holds under this set of conditions, and from further inspection of Table 2 it can be seen that there exists a general correlation between a blue–red rule in the liquid crystal system and a solubility rule in the gel system.[37]

With lyxose and xylose in certain solvents both isomers form gels, but the relative stability of the gel is not the same. The stability of the gel can be conveniently ascertained by plotting the sol–gel phase transition temperature *versus* mol% of the complex. It has become clear that L-xylose and D-lyxose have strong intermolecular interactions (blue shift in the liquid crystal system) whereas D-xylose and L-lyxose possess weak intermolecular interactions (red shift in the liquid crystal system). For further evaluation of the gel phase both scanning electron microscopy (SEM) and CD spectroscopy were performed on the gels formed with D- and L-xylose complexes. The CD spectra of the optical pairs are inverted, implying a different chirality for the gels. The SEM pictures show that open fibrous gels are formed by these complexes; twists are also clearly visible but these structures are too large for individual fibrils and so must be the result of multiple copies intertwining (super helixes). Both the CD and SEM results confirm that the cholesterol moiety is performing a similar task in the gel and liquid crystal system, holding together a chiral helix. As a corollary, this work represents a rare example of monosaccharide gelation. Also, the gelation ability of the complexes is controlled in a predictable manner by the chirality of the monosaccharide. This description of saccharide chirality is general since it is confirmed by the predictions made in the liquid crystal system.[37]

Through these studies we noticed that the CD spectra in the sol–gel transition system show very strange behaviour. We thus decided to investigate thoroughly the possible relationship between the gelation properties and the CD spectra.[36,38] As shown in Fig. 4, the spectra for **10Me** are quite different above and below T_{gel}: the absorption maximum in the isotropic solution phase (360 nm) shifts to shorter wavelength (high energy region) in the gel phase (310 nm). This means that the excited state of the azobenzene chromophore is destabilised by molecular aggregation. Interestingly, the strong CD spectrum appears only in the gel phase. The

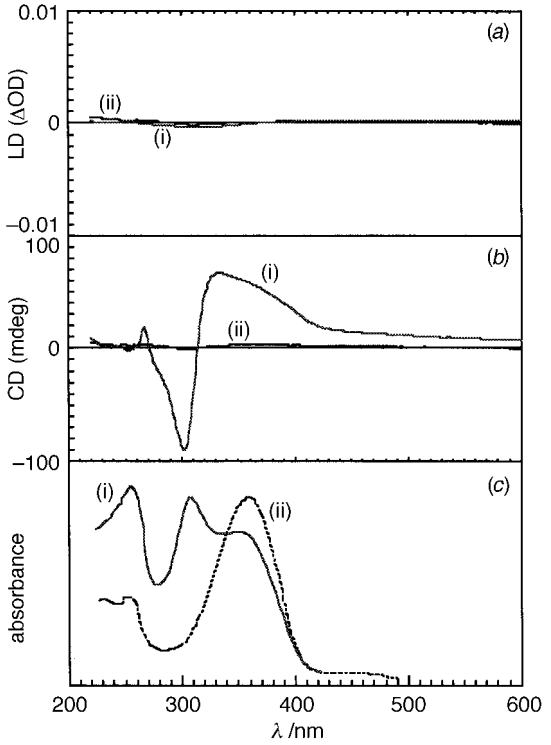

Fig. 4 (*a*) Linear dichroism (LD) spectra, (*b*) CD spectra and (*c*) absorption spectra for **10Me** (0.2 mass%) in *n*-butanol: (i) the gel state was observed at 25 °C and (ii) the solution state was observed at 60 °C

CD spectrum shows a positive exciton coupling which consists of the positive first Cotton effect and the negative second Cotton effect, and the wavelength (310 nm) at $[\theta] = 0$ agrees with the λ_{max} of the absorption maximum obtained in the gel phase. In the cholesterol gel systems (**8**, **10R**, **11R**, **12R** and **13R**), the solutions were totally CD-silent in the sol phase whereas the clear exciton coupling band appeared in the gel phase. These results suggest that in the gel phase cholesterol moieties aggregate in a specific, chiral direction, which enforces azobenzene chromophores to interact in an asymmetric manner. The drastic spectral changes are induced by the sol–gel phase transition, which can be readily 'read-out' as a change of CD spectra.

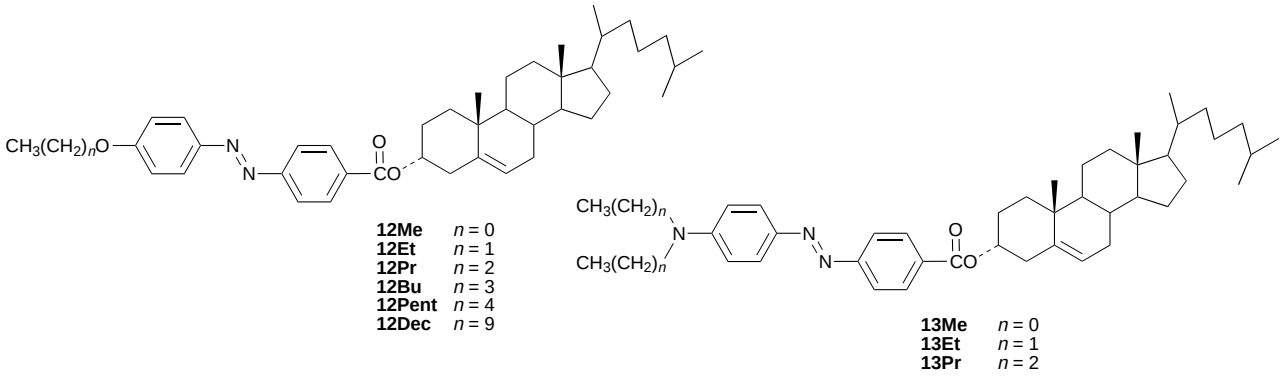

The spectral features which are the sign of CD spectra or the shifts of the absorption spectra are influenced by specific structural features, such as the absolute configuration at C-3 of a steroidal skeleton. The absolute configuration at C-3 of **8**, **10R** and **11R** is retained as the natural cholesterol β-configuration [(*S*)-chirality], whereas that of **12R** and **13R** is the inverted α-configuration [(*R*)-chirality]. In general, the natural (*S*)-C-3 derivatives have a tendency to give the positive exciton CD spectra independent of solvents, and the λ_{max} of the absorption spectra shifts to the high energy region by the sol–gel phase transition. On the other hand, the inverted (*R*)-C-3 derivatives induce no energy shifts in the absorption spectra, but the sign of the CD spectra is dependent on the solvent. The positive exciton coupling was favoured in polar solvents whereas the negative exciton coupling was favoured in nonpolar solvents. Fig. 5 shows energy-minimised structures of **10Me** and **12Me** (the α epimer of **10Me**). **12Me** with the inverted configuration at C-3 adopts an L-shaped bent conformation, whereas **10Me** with the natural configration at C-3 adopts an extended conformation which is apparently more aggregative than that of **12Me**. In the gel system, the natural derivatives showed a much stronger cohesive nature than the inverted derivatives (in melting point, liquid crystallinity, solubility and T_{gel}).[36] It is also expected that this structural difference would be reflected by the difference in the spectral properties.

Interestingly, the sign of the CD spectra is sometimes inverted depending upon the cooling speed of gelatinisation. In the **13Me**–methylcyclohexane gel, for example, the cooling of the solution (60 °C) in water at 30 °C (slow cooling) gave a negative exciton CD spectrum whereas the cooling in water at 2 °C (rapid cooling) gave a positive exciton CD spectrum. When the gel with (*R*)-chirality was gradually heated, the sign changed from (*R*) to (*S*) at around 27 °C. When the gel with (*S*)-chirality was gradually cooled to −10 °C, the θ values were increased in the negative direction and inversion of the sign did not take place. The results indicate that, basically, the **13Me** gel with (*S*)-chirality is more stable than that with (*R*)-chirality. In other words, the gel with (*R*)-chirality is a metastable phase formed by rapid cooling.

The results support the view that azobenzene-appended cholesterol-based gelators aggregate in an asymmetric manner. In particular, the appearance of the exciton coupling band in CD spectroscopy substantiates the fact that these aggregates possess a helical structure. As expected, from SEM or optical microscopy, the fibrillar aggregates, which include a helical structure, can be observed in the gel [Fig. 6(*a*)], and the crystals which were grown from the gel phase also include a clear helical structure [Fig. 6(*b*)]. Interestingly, the chirality of the CD spectra agreed with the chirality of the helical structure observed by microscopy. We now consider that cholesterol-based gels are constructed by one-dimensional helical stacking.

Recently, molecular recognition using a complementary hydrogen-bonding network between hosts and guests has become an active area of endeavour. This concept has been

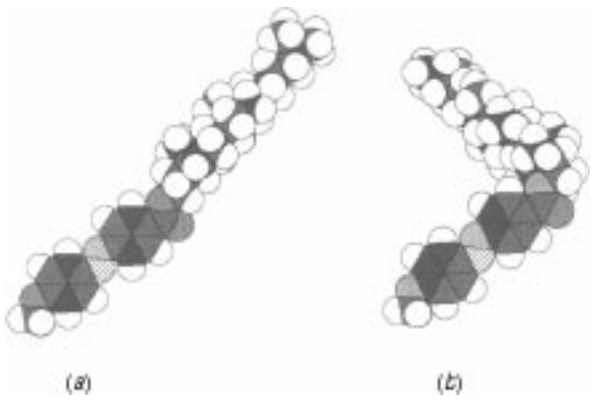

Fig. 5 Energy-minimised structures of (*a*) **10Me** with (*S*)-chirality and (*b*) **12Me** with (*R*)-chirality

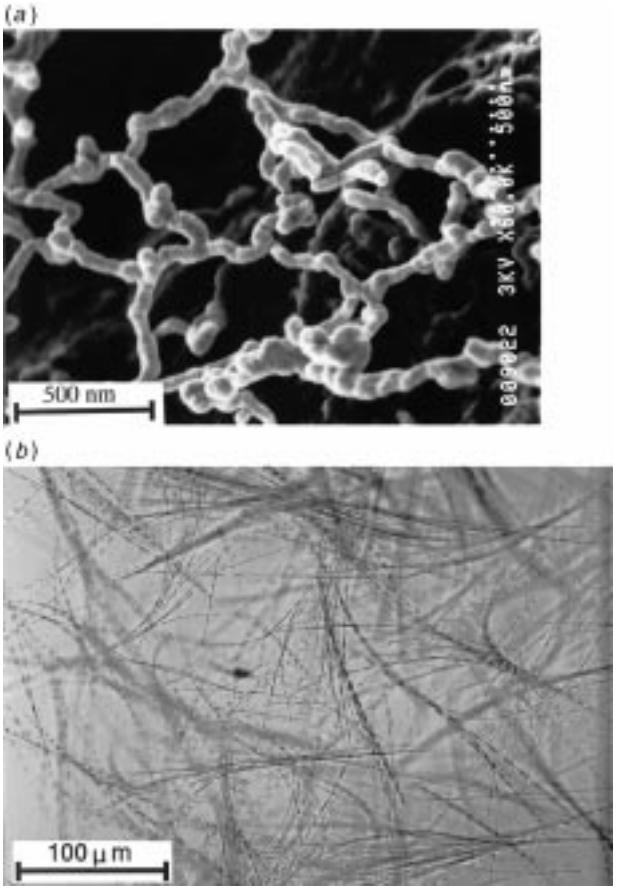

Fig. 6 (*a*) SEM picture of the dried gel for a **13Me**–cyclohexane system: the gel was prepared by slow cooling: the fibrils have a left-handed helical structure whereas the CD showed a negative exciton coupling band in this gel system. (*b*) Optical microscope picture of the fibrous crystal for **10Me**: the crystal was grown from the **10Me**–*n*-octanol gel.

applied to the formation of stable organic gels.[39–43] It seemed that if the hydrogen-bonding interaction acts cooperatively with the cholesterol–cholesterol interaction, the synergistic effect may create 'super-gelators' which can gelatinize organic solvents at very low gelator concentrations. To test this idea compounds **14** and **15** were synthesized.[44] Although **14** could gelatinize several organic solvents by itself, **15** always resulted in precipitates from these solvents. In contrast, a 1:1 **14**+**15** mixture gave reinforced organic gels because of the action of their complementary hydrogen-bonding sites.[44] It was shown, however, that the IR spectrum of the **14**+**15** gel is very complicated (*e.g.* there are many NH_2 and C=O stretching bands). When the mixture was thoroughly dissolved and then cooled very slowly, it gave a crystalline precipitate, the IR spectrum of which was more simplified than that of the gelled mixture. We now consider, therefore, that the gelled mixture does not involve a neat tape structure (as shown in Fig. 7[39c]) but a partially disordered, kinetically stable structure.

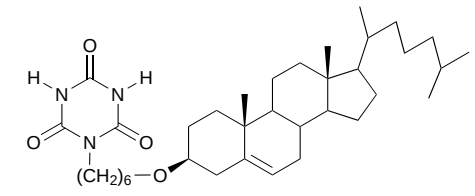

14

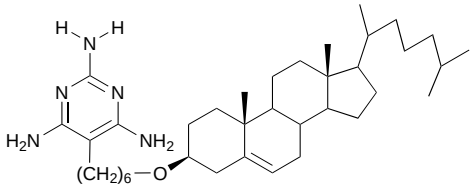

15

Organic gels have been considered to be troublesome systems to which neither conventional recrystallisation nor spectroscopic analysis can be applied. As reviewed in this section, however, prerequisites for organic gel formation have been elucidated and it has been shown that gelators assemble into fibrous aggregates with an oriented structure in organic solvents, reflecting the molecular shape and the intermolecular interaction mode: chiral gelators such as cholesterol derivatives tend to form helical structures and hydrogen-bonding gelators tend to aggregate so that they can satisfy complementary donor–acceptor interactions. We believe that gel systems are an under-exploited field which has great potential for molecular recognition and switch functions and by which one can create a number of new three-dimensional molecular assemblies. Cholesterol derivatives would play a central role in such gel systems because of their versatility.

Monolayer systems

Recently, great interest has developed around the application of monolayers formed at the air–water interface to molecular recognition.[45–47] Of particular interest is the potential application to chiral discrimination: chiral guest molecules in the subphase interact with chiral amphiphilic compounds forming the monolayer and the resultant 'diastereomeric complexes' change the surface-pressure (π–A) isotherm in an asymmetric manner.[48,49] It was recently demonstrated that certain cholesterol derivatives (such as **1**, **2** and **6a**) form beautiful monolayers.[50] Judging from the π–A curves, the crown ether moieties, which tend to spread on the water surface and adopt a parallel orientation, stand up gradually with increasing surface pressure and are finally packed as a monolayer with a vertical orientation. Interestingly, the π–A isotherms responded specifically to added alkali metal cations because of the metal–crown interaction.[50]

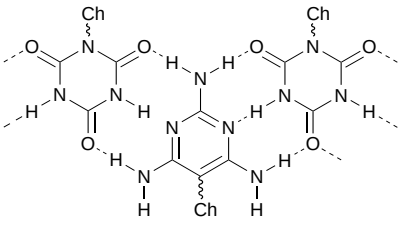

Fig. 7 Tape structure with complementary hydrogen-bonding interactions between a triaminopyrimidine unit and an isocyanuric acid: Ch denotes a cholesterol moiety

It occurred to us that this system may be applicable to chiral discrimination of α-amino acid derivatives because the 18-crown-6 moiety in **1b** should bind the NH_3^+ group also at the air–water interface. Addition of D-PheOMe·HCl (D-phenylalanine methyl ester hydrochloride) to a subphase under a monolayer of **1b** induced a large expansion of the monolayer; when L-PheOMe·HCl was added only a small expansion occurred. Chiral discrimination was also achieved for other α-amino acid derivatives (Table 3), but the largest effect was observed with PheOMe·HCl. Why is such chiral discrimination of α-amino acid derivatives, which is difficult with conventional chiral amphiphilic compounds, readily realised in a cholesterol-based monolayer system? It is certain that the NH_3^+ moiety is bound to the 18-crown-6 ring. As the α-amino acid residue CH_2R is more hydrophobic than the CO_2Me group, this group should be trapped in the hydrophobic cholesterol stacks. In this binding mode, the cholesterol skeleton with a wide chiral plane can more advantageously constrain the orientation of α-amino acid derivatives than conventional chiral amphiphiles with simple point chirality. Thus, the α-amino acid derivatives are recognised at two points (NH_3^+ by the crown ring and CH_2R by the cholesterol plane) by a monolayer of **1b**.

We previously found that cholesteric liquid crystals containing **1b** can asymmetrically recognise α-amino acid derivatives: L-isomers stabilise the liquid crystal phase to shorten the pitch length whereas D-isomers destabilise the liquid crystal phase to elongate the pitch length.[10] Although the monolayer phase is different from the liquid crystal phase, the microscopic environments where one amino acid residue is flanked by two cholesterol planes should be similar to each other. Important is the fact that in both systems D-isomers disorder the cholesterol-based oriented phases more efficiently than L-isomers. Presumably, the space formed between two cholesterols fits the asymmetric shape of L-isomers more complementarily than that of D-isomers.

The relationship between molecular structure and physical properties of monolayers of complexes between an amphiphilic, cholesterol-substituted phenylboronic acid **3** and monosaccharides were studied at the air–water interface.[51] Phase transition, compressibility and limiting molecular area of monolayers of **3** in the presence of monosaccharides are correlated with the calculated structures of the phenylboronic acid–monosaccharide complexes. The monolayer of **3** exhibits

Table 3 Limiting area A_0 and lift-off area A_1 of **1b** on 100 mM amino acid methyl ester hydrochlorides

	A_0/nm^2 molecule^{-1}		A_1/nm^2 molecule^{-1}	
amino acid	L-isomer	D-isomer	L-isomer	D-isomer
Phe	0.72	0.91	1.06	1.44
Ala	0.82	0.79	1.20	1.44
Trp	0.81	0.84	1.34	1.33
Val	0.71	0.77	1.04	1.14

chiral discrimination towards optical isomers of monosaccharides.[51] As explained above for liquid crystals of **3**–saccharide complexes, most monosaccharides form 2:1 complexes with the pyranose form in non-aqueous media (see Scheme 1), from which the Ph–Ph angle for the most stable structures was theoretically computed.[11] In this system the boron atom is sp^2-hybridised. In contrast to that in non-aqueous systems, monosaccharides preferably exist as furanoses in boronic acid complexes in aqueous alkaline bulk solution, where the boron atom is sp^3-hybridised.[52] Furthermore, it is uncertain whether **3** forms similar 2:1 complexes. To solve these complex problems at the air–water interface we first determined the stoichiometry by using a mass spectrometer. A built-up film of 80 layers of an amphiphilic phenylboronic acid on a subphase containing D-glucose at pH 11 was prepared by vertical dipping of a steel plate. The mass spectrum of the sample thus collected supported the double-charged 2:1 complex (Fig. 8).[53] We could not solve the furanose *vs.* pyranose problem, however. For the present study, therefore, the following two series of calculations were taken into account for model compounds of all experimentally studied monosaccharide complexes of **1** in order to determine their water-facing angle (Fig. 9): (*i*) sp^2-hybridised boron and pyranoses, because these complexes are most stable in non-aqueous solvents and the air–water interface provides an environment distinct from the aqueous bulk solution and (*ii*) sp^3-hybridised boron atom and furanoses, because these complexes are more stable in aqueous alkaline solution and the pH of the subphase is higher than pK_a (pK_a *ca.* 9). The calculations are shown in Table 4.

It is seen from Fig. 10 that the complexes are clearly divided into two groups according to their structure. Those causing a red shift in the cholesteric liquid crystal system and destabilising it (D-xylose, L-mannose, L-arabinose, D-fucose, D-glucose and D-allose) fit a linear plot in Fig. 10(*a*), while those causing a blue shift in the same system and stabilising it (L-xylose, D-fructose, D-galactose, D-mannose, D-arabinose, L-fucose and L-glucose) fit a linear plot in Fig. 10(*b*). A remarkable correlation between monolayer property and molecular structure is observed: the smaller the angle α between two intramolecular cholesterol moieties, the lower the transition pressure. The

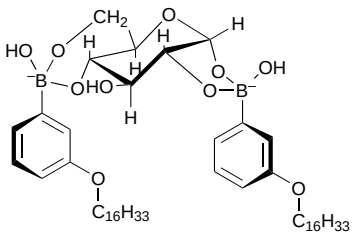

Fig. 8 2:1 complex with sp^3-hybridised borons formed at the air–water interface. The complex structure is illustrated assuming the pyranose form.

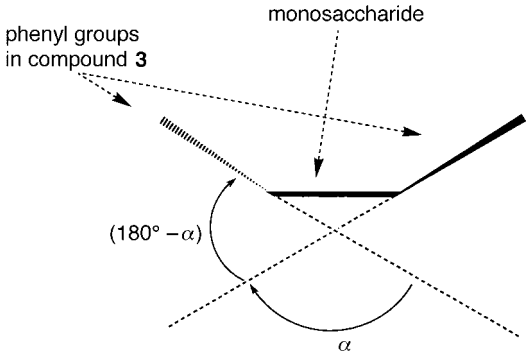

Fig. 9 Relationship between the Ph–Ph angle and the water-facing angle α.

Table 4 Water-facing angles of the complexes between **3** and monosaccharides in the pyranose or furanose form for the MO-optimised structures

saccharide	binding site	calculated angle of pyranose complexes	binding site	calculated angle of furanose complexes
xylose	1,2–3,4	153.5	1,2–3,5	93.2
fructose	2,3–4,5	143.3	1,2–4,6	115.3
galactose	1,2–4,6	134.6	1,2–5,6	132.3
mannose	2,3–4,6	131.6	2,3–5,6	166.7
arabinose	1,2–3,4	126.9	1,2–3,5	103.5
fucose	1,2–3,4	123.3	1,2–3,5	100.9
glucose	1,2–4,6	95.8	1,2–5,6	145.5
allose	2,3–4,6	95.6	2,3–5,6	119.1

monolayers of complexes with a small water-facing angle α such as the glucose complex require a lower surface pressure to achieve the phase transition and to rearrange both the structure of the complex and packing in the monolayer compared with complexes with a larger angle α, *e.g.* with fructose. Alternatively, we also tried to correlate the transition pressure with the angle for the complexes with furanose-type monosaccharides with the boron atom sp^3-hybridised,[51] because in aqueous bulk solution monosaccharides adopt this form in boric acid complexes.[52] However, there is no correlation between transition pressure and the water-facing angle for the furanose complexes. The difference in correlation suggests that the pyranose form is predominant under the experimental conditions. The monolayer must provide an environment unlike the bulk aqueous solution. This finding is in agreement with the previously proposed reduced solvating capability of water molecules near the air–water interface.[54]

The monolayer formation properties of cholesterol-based azobenzene amphiphiles with the natural (*S*)-C-3 configuration (**10Me**) and inverted (*R*)-C-3 configuration (**12Me**) were examined at the air–water interface.[55] The close correlation between the gel system and the monolayer system was observed here again. The computational study reveals that **10Me** adopts an extended conformation whereas **12Me** adopts an L-shaped bent conformation.[36] **10Me** gave an expanded phase with A_0 (limiting area) = 0.60 nm^2 $molecule^{-1}$ and A_1 (lift-off area) = 0.64 nm^2 $molecule^{-1}$ whereas **12Me** gave a condensed phase with $A_0 = 0.49$ and $A_1 = 0.54$ nm^2 $molecule^{-1}$. Examination using reflectance spectroscopy established that **12Me** forms a monolayer with a J-aggregation mode (λ_{max} 407 nm) and with an increase in the compressibility it changes to an H-aggregation mode (λ_{max} 336 nm). The finding indicates that the azobenzene moieties interact with each other although the aggregation mode is dependent on the compressibility. This spectroscopic character is very similar to a spectral change observed for the sol–gel phase transition of **10Me** gels.[36,38] On the other hand, **12Me** forms a monolayer having a λ_{max} (362 nm) comparable with the monomeric absorption maximum, indicating that the electronic interaction among the azobenzene moieties is absent. This trend is again very similar to the sol–gel phase transition of **12Me** gels which does not show any significant spectral change.[36,38] One can conclude, therefore, that the difference in the gel formation between **10Me** and **12Me** is well reproduced in the monolayer formation. The morphological changes in the monolayers were directly observed by optical microscopy and reasonably correlated with the spectroscopic changes. Octadecyl Rhodamine B (used as a fluorescent probe) is more miscible with **12Me** (less cohesive[36]) than with **10Me** (more cohesive[36]). This difference is reflected by the π–A isotherms: the π–A isotherm for **12Me** plus octadecyl Rhodamine B is not so different from that for **12Me** only, whereas the collapse pressure for **10Me** plus octadecyl Rhodamine B is significantly lower than that for

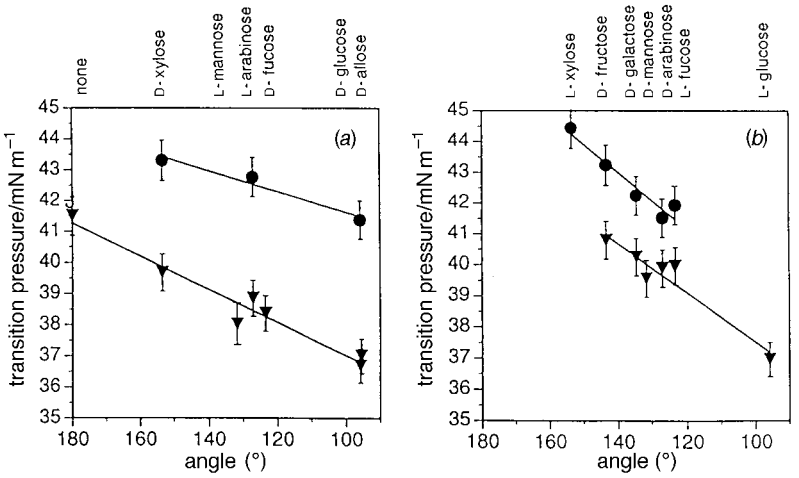

Fig. 10 Plots of surface pressure of monolayers of **3** at phase transition *vs.* water-facing angle α of the complexes which destabilise or stabilise the cholesteric liquid crystal; ● at 293 K, and ▼ at 303 K

10Me only. The domain structure was not observed immediately after spreading a benzene solution containing **12Me**, but after a few minutes the domain structure appeared. From reflectance spectroscopy we noticed that the reflectance intensity fluctuates with time above A_1. Optical microscopy suggests that the microaggregates of **12Me** are drifting on the water surface, and the reflectance intensity increases when they come into the vision field of the microscope. The findings support the view that **12Me** also forms the microaggregates even at 0 mN m^{-1}. At $\pi = 19.0$ mN m^{-1} (just below π_c), a large, nearly homogeneous monolayer of **12Me** was observable. At $\pi > \pi_c$, on the other hand, long stripes appeared in the homogeneous domain. These wrinkles are formed by a compression that is strong enough to collapse the monolayer. On the other hand, **10Me** gave a number of bright spots above A_1. As demonstrated by reflectance spectroscopy, this pattern corresponds to the formation of microaggregates with a J-aggregation mode. When they are compressed to a monolayer, one can observe a well-dispersed island structure. This corresponds to an expanded monolayer phase with a J-aggregation mode. Further increase in the compression changed the island structure to a network structure with large cracks. Conceivably, the monolayer is collapsed here and a crystal (or liquid crystal) with an H-aggregation mode is produced on the surface.

The monolayer system is different from the liquid crystal system and the gel system in the following two ways: it is an event occurring in a two-dimensional domain and the parameters obtained from the condensed subphase more or less reflect those of the crystal phase. In cholesterol-based amphiphiles, however, the parameters and their perturbation induced by guests added into the subphase are surprisingly similar to each other. The results imply that the aggregation mode in these systems is primarily governed by a cholesterol moiety which inherently possesses an aggregative tendency, whereas appended functional groups play only a secondary role in the structural orientation.

Conclusions

The main purpose of the present feature article is to demonstrate that cholesterol derivatives (or more generally, steroids) act as versatile building-blocks commonly useful for the formation of liquid crystals, organic gels and monolayers. Through these studies it has been shown that (*i*) cholesterol can provide chiral and moderately rigid platforms for molecular orientation and molecular recognition, (*ii*) although the aggregation modes are restricted by boundary conditions inherent to each phase, one can raise many correlation relationships among different phases, *e.g.* in guest selectivity, cohesivity, phase transition, spectroscopic properties, *etc.* and (*iii*) a slight change in the cholesterol structure leads to a large change in the aggregation properties, which is characteristic of molecular assembly systems. We have noticed that in these systems, it is essential to obtain an insight into the relation between the aggregation mode of the cholesterol moieties and that of the functional groups appended to their 3-OH. The packing mode of cholesterol derivatives in the crystal state has been studied by several groups.[56–60] However, the relation between the cholesterol structure and the packing mode is not yet well correlated[60] and to simply predict the aggregation mode of metastable and partially-disordered phases mentioned in this article from the X-ray-determined single-crystal structure is not appropriate. Probably, one has to find some alternative approach to this problem. On the other hand, recent studies have shown that crystals derived from steroid derivatives can provide novel crystal lattices and inclusion compounds.[61] This suggests that they are also useful as a part of molecular tectonics. We believe that cholesterol-based molecular assembly systems can be further extended as novel molecular orientation systems to chiral molecular recognition, molecular switches, controlled electron or energy transfer systems, membrane separations, *etc.*

References

1 (*a*) E. B. Kyba, K. Koga, L. R. Sousa, M. G. Siegel and D. J. Cram, *J. Am. Chem. Soc.*, 1973, **95**, 2692; (*b*) Y. Chao and D. G. Cram, *J. Am. Chem. Soc.*, 1976, **98**, 1015; (*c*) D. J. Cram, R. C. Hegelson, L. R. Sousa, J. M. Timko, M. Newcomb, P. Moreau, F. de Jong, G. W. Gokel, D. H. Hoffman, L. A. Domier, S. C. Peacock, K. Madan and L. Kaplan, *Pure Appl. Chem.*, 1975, **43**, 327; (*d*) M. Newcomb, J. L. Toner, R. C. Helgeson and D. J. Cram, *J. Am. Chem. Soc.*, 1979, **101**, 4941; (*e*) J.-M. Lehn and C. Sirlin, *J. Chem. Soc., Chem. Commun.*, 1978, **143**; (*f*) J.-M. Lehn, *Science,* 1985, **227**, 849.

2 For applications of steroidal compounds in supramolecular chemistry see: (*a*) A. P. Davis, *Chem. Soc. Rev.*, 1993, **22**, 243 (and references cited therein); (*b*) R. P. Bonar-Law and J. K. M. Sanders, *J. Am. Chem. Soc.*, 1995, **117**, 259; (*c*) H.-P. Hsieh, J. G. Muller and C. J. Burrows, *J. Am. Chem. Soc.*, 1994, **116**, 12077; (*d*) Y. A. Cheng, T. Suenaga and W. C. Still, *J. Am. Chem. Soc.*, 1996, **118**, 1813; (*e*) V. Janout, M. Lanier and S. L. Regen, *J. Am. Chem. Soc.*, 1996, **118**, 1573; (*f*) U. Maitra and L. J. D'Souza, *J. Chem. Soc., Chem. Commun.*, 1994, 2793; (*g*) P. Venkatasan, Y. Cheng and D. Kahne, *J. Am. Chem. Soc.*, 1994, **116**, 6955; (*h*) A. P. Davis and J. J. Walsh, *J. Chem. Soc., Chem. Commun.*, 1996, 449; (*i*) A. P. Davis, S. Menzer, J. J. Walsh and D. J. Williams, *Chem. Commun.*, 1996, 453.

3 For example, see (*a*) T. Kaneda, K. Hirase and S. Misumi, *J. Am. Chem. Soc.*, 1989, **111**, 742; (*b*) K. Yamamoto, K. Isoue, Y. Sakata and T. Kaneda, *J. Chem. Soc., Chem. Commun.*, 1992, 791;

(*c*) Y. Kubo, S. Maeda, S. Tokita and M. Kubo, *Nature*, 1996, **382**, 522.
4 For chiral recognition in liquid crystal systems see: (*a*) C. Eskenazi, J. F. Nicoud and H. B. Kagan, *J. Org. Chem.,* 1979, **44**, 995; (*b*) F. D. Saeva, P. E. Sharpe and G. R. Olin, *J. Am. Chem. Soc*., 1975, **97**, 204. For regioselectivity control in liquid crystal systems see: (*c*) J. M. Nerbonne and R. G. Weiss, *J. Am. Chem. Soc*., 1978, **100**, 2571; (*d*) T. Nagamatsu, C. Kawano, Y. Orita and T. Kunieda, *Tetrahedron. Lett*., 1978, **28**, 3263; (*e*) W. J. Leigh and D. S. Mitchell, *J. Am. Chem. Soc.,* 1988, **110**, 1311.
5 For the use of thermotropic liquid crystals as solvents see; R. G. Weiss, *Tetrahedron,* 1988, **44**, 3413.
6 G.-X. He, F. Wada, K. Kikukawa, S. Shinkai and T. Matsuda, *J. Org. Chem*., 1990, **55**, 541, 548.
7 (*a*) G. W. Gokel, J. C. Hernandez, A. M. Viscariello, K. A. Arnold, C. F. Champana, L. Echegoyen, F. R. Fronczek, R. D. Gandour, C. R. Morgan, J. E. Trafton, S. R. Miler, C. Minganti, D. Eiband, R. A. Schultz and M. Tamminen, *J. Org. Chem*., 1987, **52**, 2963; (*b*) L. E. Echegoyen, L. Portugal, S. R. Miller, J. C. Hernandez, L. Echegoyen and G. W. Gokel, *Tetrahedron Lett*., 1988, **29**, 4065; (*c*) L. E. Echegoyen, J. C. Hernandez, A. E. Kaifer, G. W. Gokel and L. Echegoyen, *J. Chem Soc., Chem. Commun*., 1988, 836.
8 S. Shinkai, T. Nishi, A. Ikeda, T. Matsuda, K. Shimamoto and O. Manabe, *J. Chem. Soc., Chem. Commun*., 1990, 303.
9 S. Shinkai, T. Nishi and T. Matsuda, *Chem. Lett*., 1991, 437.
10 T. Nishi, A. Ikeda, T. Matsuda and S. Shinkai, *J. Chem. Soc., Chem. Commun*., 1991, 339.
11 T. D. James, T. Harada and S. Shinkai, *J. Chem. Soc., Chem. Commun*., 1993, 857 and 1176 (corrigendum)
12 (*a*) S. Shinkai, K. Tsukagoshi, Y. Ishikawa and T. Kunitake, *J. Chem. Soc., Chem. Commun*., 1991, 1039; (*b*) K. Tsukagoshi and S. Shinkai, *J. Org. Chem*., 1991, **56**, 4089; (*c*) K. Kondo, Y. Shiomi, M. Saisho, T. Harada and S. Shinkai, *Tetrahedron*, 1992, **48**, 8239.
13 (*a*) G. Wulff, B. Heide and G. Helfmeier, *J. Am. Chem. Soc*., 1986, **108**, 1089; (*b*) G. Wulff and H.-G. Poll, *Makromol. Chem*., 1987, **188**, 741.
14 (*a*) T. Kajiyama, H. Kikuchi and S. Shinkai, *J. Membr. Sci*., 1988, **36**, 243; (*b*) T. Kajiyama, S. Washizu, A. Kumano, I. Terada, M. Takayanagi and S. Shinkai, *J. Appl. Polym. Sci., Appl. Polym. Symp*., 1985, **41**, 327.
15 (*a*) S. Shinkai, S. Nakamura, S. Tachiki, O. Manabe and T. Kajiyama, *J. Am. Chem. Soc*., 1985, **107**, 3363; (*b*) S. Shinkai, S. Nakamura, K. Ohara, S. Tachiki, O. Manabe and T. Kajiyama, *Macromolecules*, 1987, **20**, 21.
16 (*a*) S. Shinkai, K. Torigoe, O. Manabe and S. Shinkai, *J. Chem. Soc., Chem. Commun*., 1986, 933; (*b*) *J. Am. Chem. Soc*., 1987, **109**, 4458.
17 S. Shinkai, K. Shimamoto, O. Manabe and M. Sisido, *Makromol. Chem., Rapid Commun*., 1989, **10**, 361.
18 S. Shinkai, G.-X. He, T. Matsuda, K. Shimamoto, N. Nakashima and O. Manabe, *J. Polym. Sci., Polym. Lett. Ed*., 1989, **27**, 209.
19 S. Shinkai, T. Nishi, K. Shimamoto and O. Manabe, *Is. J. Chem*., 1992, **32**, 121.
20 U. F. Kragten, M. F. M. Roks and J. M. Nolte, *J. Chem. Soc., Chem. Commun*., 1985, 1275.
21 S. B. Hladky and D. A. Haydon, *Biochim. Biophys. Acta*, 1972, **274**, 294.
22 M. Sirai, T. Orikata and M. Tanaka, *J. Polym. Sci., Polym. Chem. Ed*., 1985, **23**, 463.
23 J. Donis, J. Grandjean, A. Grosjean and P. Lazlo, *Biochim. Biophys. Acta*, 1981, **102**, 690 and references cited therein.
24 H. Tokuhisa, K. Kimura, M. Yokoyama and S. Shinkai, *J. Chem. Soc., Faraday Trans*., 1995, **91**, 1237.
25 Y.-C. Lin and R. G. Weiss, *Macromolecules,* 1987, **20**, 414.
26 Y.-C. Lin, B. Kachar and R. G. Weiss, *J. Am. Chem. Soc.,* 1989, **111**, 5542.
27 Y.-C. Lin and R. G. Weiss, *Liquid Crystals,* 1989, **4,** 367 and references cited therein.
28 R. Mukkamala and R. G. Weiss, *J. Chem. Soc., Chem. Commun*., 1995, 375.
29 E. Ostuni, P. Kamaras and R. G. Weiss, *Angew. Chem., Int. Ed. Engl*., 1996, **35**, 1234.
30 L. Lu and R. G. Weiss, *Langmuir*, 1995, **11**, 3630.
31 (*a*) P. Terech, *J. Colloid Interface Sci*., 1985, **107**, 244; (*b*) R. H. Wade, P. Terech, E. A. Hewat, R. Ramasseul and F. Volino, *J. Colloid Interface Sci*., 1986, **114**, 442.
32 P. Terech, *Liquid Crystals*, 1991, **9**, 59.
33 (*a*) T. Brotin, R. Utermöhlen, F. Fages, H. Buas-Laurent and J.-P. Desvergne, *J. Chem. Soc., Chem. Commun*., 1991, 416; (*b*) T. Brotin, J.-P. Desvergne, F. Fages, R. Utermöhlen, R. Bonneau and H. Bouas-Laurent, *Photochem. Photobiol*., 1992, **55**, 349.
34 For a comprehensive review see T. D. James, H. Kawabata, R. Ludwig, K. Murata and S. Shinkai, *Tetrahedron*, 1995, **51**, 555.
35 K. Murata, M. Aoki, T. Nishi, A. Ikeda and S. Shinkai, *J. Chem. Soc., Chem. Commun*., 1991, 1715.
36 K. Murata, M. Aoki, T. Suzuki, T. Harada, H. Kawabata, T. Komori, F. Ohseto, K. Ueda and S. Shinkai, *J. Am. Chem. Soc*., 1994, **116**, 6664.
37 T. D. James, K. Murata, T. Harada, K. Ueda and S. Shinkai, *Chem. Lett*., 1994, 273.
38 K. Murata, M. Aoki and S. Shinkai, *Chem. Lett*., 1992**,** 739.
39 (*a*) K. Hanabusa, K. Okui, K. Karaki, T. Koyama and H. Shirai, *J. Chem. Soc., Chem. Commun*., 1992, 1371; (*b*) K. Hanabusa, M. Yamada, M. Kimura and H. Shirai, *Angew. Chem. Int. Ed. Engl*., 1996, **35**, 1949; (*c*) K. Hanabusa, T. Miki, Y. Taguchi, T. Koyama and H. Shirai, *J. Chem. Soc., Chem. Commun*., 1993, 1382.
40 (*a*) N. A. J. M. Sommerdijk, M. H. L. Lambermon, M. C. Feiters, R. J. M. Nolte and B. Zwanenburg, *Chem. Commun*., 1997, 455; (*b*) R. J. H. Hafkamp, B. P. A. Kokke, I. M. Danke, H. P. M. Geurts, A. E. Rowan, M. C. Feiters and R. J. M. Nolte, *Chem Commun*., 1997, 545.
41 E. J. de Vries and R. M. Kellogg, *J. Chem. Soc., Chem. Commun*., 1993, 238.
42 M. Takafuji, H. Ihara, C. Hirayama, H. Hachisako and K. Yamada, *Liquid Crystals*, 1995, **18**, 97.
43 J.-E. Sohna and F. Fages, *Chem. Commun*., 1997, 327.
44 S. W. Jeong, K. Murata and S. Shinkai, *Supramol. Sci*., 1996, **3**, 83.
45 (*a*) K. Kurihara, K. Ohto, Y. Tanaka, Y. Aoyama and T. Kunitake, *J. Am. Chem. Soc*., 1991, **113**, 444; (*b*) K. Kurihara, K. Ohto, Y. Honda and T. Kunitake, *J. Am. Chem. Soc*., 1991, **113**, 5077; (*c*) Y. Ikeura, K. Kurihara and T. Kunitake, *J. Am. Chem. Soc*., 1991, **113**, 7342.
46 Y. Ishikawa, T. Kunitake, T. Matsuda, T. Otsuka and S. Shinkai, *J. Chem. Soc., Chem. Commun*., 1989, 1937.
47 H. Kawabata and S. Shinkai, *Chem. Expr*., 1993, **8**, 765.
48 (*a*) E. M. Arnett, N. G. Harvey and P. L. Rose, *Acc. Chem. Res*., 1989, **22**, 131; (*b*) N. G. Harvey, D. Mirajovsky, P. L. Rose, R. Verbiar and E. M. Arnett, *J. Am. Chem. Soc*., 1991, **111**, 1115.
49 P. Qian, M. Matsuda and T. Miyashita, *J. Am. Chem. Soc*., 1993, **115**, 5624.
50 T. Nishi and S. Shinkai, *Chem. Expr*., 1993, **8**, 173.
51 R. Ludwig, T. Harada, K. Ueda, T. D. James and S. Shinkai, *J. Chem. Soc., Perkin Trans.* **2**, 1994, 697.
52 (*a*) S. Chapelle and J.-F. Verchere, *Tetrahedron,* 1988, **44,** 4469; (*b*) J. C. Norrild and H. Eggert, *J. Am. Chem. Soc*., 1995, **117**, 1479.
53 R. Ludwig, K. Ariga and S. Shinkai, *Chem. Lett*., 1993, 1413.
54 Y. Honda, K. Kurihara and T. Kunitake, *Chem. Lett*., 1991, 681.
55 H. Kawabata, K. Murata, T. Harada and S. Shinkai, *Langmuir*, 1995, **11**, 623.
56 B. M. Craven and G. T. DeTitta, *J. Chem. Soc., Perkin Trans. 2*, 1976, 814.
57 N. G. Guerina and B. M. Craven, *J. Chem. Soc., Perkin Trans. 2*, 1979, 1414.
58 H.-S. Shieh, L. G. Hoard and C. E. Nordman, *Acta Crystallogr. Sect. B*., 1981, **37**, 1538.
59 H.-P. Weber, B. M. Craven and P. Sawzik, *Acta. Crystallogr. Sect. B*., 1991, **47**, 116.
60 E. Otsuni, P. Kamaras and R. G. Weiss, *Angew. Chem., Int. Ed. Engl*., 1996, **35**, 1324.
61 For a comprehensive review see M. Miyata and K. Sada, *Comprehensive Supramolecular Chemistry*, ed. J.-M. Lehn, Pergamon Press, London, 1996, p. 147.

Paper 7/04820C; *Received* 7*th July*, 1997